0022-3565/00/2932-0646$03.00/0
THE JOURNAL OF PHARMACOLOGY AND EXPERIMENTAL THERAPEUTICS
Vol. 293, No. 2
Printed in U.S.A.

JPET 293:646–653, 2000 /2072/820842

Pharmacokinetic-Pharmacodynamic Modeling of the Antinociceptive Effects of Main Active Metabolites of Tramadol, (+)-*O*-Desmethyltramadol and (−)-*O*-Desmethyltramadol, in Rats[1]

MARTA VALLE,[2] MARÍA J. GARRIDO,[3] JUAN M. PAVÓN, ROSARIO CALVO, and IÑAKI F. TROCÓNIZ

Department of Pharmacology, School of Medicine, University of Basque Country, Leioa, Bizkaia (M.V., M.J.G., J.M.P, R.C.); and Department of Pharmacy and Pharmaceutical Technology, Faculty of Pharmacy, University of Navarra, Pamplona (I.F.T.), Spain

Accepted for publication January 31, 2000 This paper is available online at http://www.jpet.org

ABSTRACT

The pharmacokinetics and pharmacodynamics of the two main metabolites of tramadol, (+)-*O*-desmethyltramadol and (−)-*O*-desmethyltramadol, were studied in rats. Pharmacodynamic endpoints evaluated were respiratory depression, measured as the change in arterial blood pCO_2, pO_2, and pH levels; and antinociception, measured by the tail-flick technique. The administration of 10 mg/kg (+)-*O*-desmethyltramadol in a 10-min i.v. infusion significantly altered pCO_2, pO_2, and pH values in comparison with baseline and lower-dose groups ($P < .05$). However, 2 mg/kg administered in a 10-min i.v. infusion was enough to achieve 100% antinociception without respiratory depression. Moreover, the β-funaltrexamine pretreatment completely eliminated the antinociception of the 2-mg/kg dose, suggesting that such an effect is due to μ-opioid receptor activation. To describe and adequately characterize the in vivo antinociceptive effect of the drug, (+)-*O*-desmethyltramadol was given at different infusion rates of varying lengths (10–300 min). Pharmacokinetics was best described by a two-compartmental model. The time course of response was described using an effect compartment associated with a linear pharmacodynamic model. The estimates of the slope of the effect versus concentration relationship were significantly decreased ($P < .05$) as the length of infusion was increased, suggesting the development of tolerance. Doses of up to 8 mg/kg (−)-*O*-desmethyltramadol given in 10-min i.v. infusion did not elicit either antinociception in the tail-flick test or respiratory effects. These in vivo results are in accordance with the opiate and nonopiate properties reported for these compounds in several in vitro studies.

Tramadol hydrochloride is a centrally acting analgesic drug that is widely used in the treatment of pain. It exhibits good analgesic efficacy and a potency comparable to codeine (Hummel et al., 1996; Miranda and Pinardi, 1998).

Tramadol is administered as a racemic mixture of two enantiomers, (+)-tramadol and (−)-tramadol, that are essentially metabolized by the liver (Lee et al., 1993), producing mainly the (+)-*O*-desmethyltramadol, (+)-M1, and (−)-*O*-desmethyltramadol, (−)-M1, metabolites, respectively. There is evidence that the M1 enantiomers show analgesic activity in mice and rats (Hennies et al., 1988). The fact that these four compounds [(+)- and (−)-tramadol and (+)- and (−)-M1] have different pharmacological properties (Raffa and Friderichs, 1996) makes tramadol an atypical opioid with a complex mechanism of action.

Although the opioid component of tramadol-induced antinociception was detected in early preclinical in vitro and in vivo studies, the importance of the nonopioid component has been recognized by Raffa et al. (1992). Frink et al. (1996) have demonstrated in in vitro receptor binding and synaptosomal uptake experiments that the (+)-enantiomers are bound mainly to the opioid receptor, (+)-M1 being the compound with the highest affinity for the μ-receptors; on the other hand, (−)-enantiomers had the ability to inhibit the noradrenaline (NA) uptake. Additionally, (+)-tramadol had the property of inhibiting serotonin uptake. These results have also been supported by other authors, such as Driessen et al. (1993), Sevcik et al. (1993), Lai et al. (1996), and Bamigbade et al. (1997).

Received for publication August 31, 1999.
[1] This work was supported by a grant from the University of Basque Country (026, EB 231/96). M.V. was supported by a fellowship from the University of Basque Country.
[2] Current address: Department of Biopharmaceutical Sciences, School of Pharmacy, University of California, San Francisco, CA.
[3] Current address: Department of Pharmacy and Pharmaceutical Technology, Faculty of Pharmacy, University of Navarra, Pamplona, Spain.

ABBREVIATIONS: %MPE, percentage of maximum possible effect; M1, *O*-desmethyltramadol; β-FNA, β-funaltrexamine; pk, pharmacokinetic; pd, pharmacodynamic; NA, noradrenaline; Cl, total plasma clearance; c.v., coefficients of variation.

Although several in vivo studies (Raffa et al., 1992, 1993) dealing with the role of the opioid and nonopioid components in analgesia induced by tramadol corroborate the in vitro findings (Raffa et al., 1995), there is little or no information regarding the pharmacokinetic (pk) properties of the tramadol enantiomers and their metabolites or their pharmacokinetic/pharmacodynamic (pk/pd) relationships. pk/pd studies have been used as a tool for describing and predicting the time course of the in vivo effect in different scenarios (Derendorf and Hochhaus, 1995). In the case of tramadol, the following pk and pd complexities could hamper a priori the interpretation of the time course of its effect: 1) transport to the biophase (central nervous system), 2) active metabolites, 3) pd interactions among the enantiomers and metabolites, and 4) eventual development of tolerance. For all of these reasons, in this study we approach the understanding of the in vivo effect of tramadol by characterizing first the relationship between the pk and the antinociceptive effects of its metabolites, (+)-M1 and (−)-M1. In addition, the irreversible μ-antagonist β-funaltrexamine (β-FNA) was administered to explore the role of μ-receptor in the antinociception elicited by (+)-M1 because β-FNA has been used by several authors to study the relationship between reduction in μ-receptor density and loss of agonist efficacy (Adams et al., 1990; Randich et al., 1993).

When dealing with opioid drugs, it is important to consider their capability to induce respiratory depression (Lee et al., 1993). Although tramadol has not caused clinically relevant respiratory depression within the recommended dose range (Houmes et al., 1992), no studies have been carried out to examine the respiratory effect of its main metabolites. On the basis of the above considerations, the respiratory effects of (+)-M1 and (−)-M1 were also evaluated during this study.

Materials and Methods

Chemicals

The hydrochloride salts of (+)-M1, (−)-M1, and the ethoxy analog of tramadol (used as an analytical internal standard) were kindly supplied by Grünenthal GmbH (Aachen, Germany). β-FNA was purchased from Tocris Cookson Ltd. (Bristol, United Kingdom). All reagents and solvents used were purchased from commercial sources and were of analytical grade.

Animals

Male Sprague-Dawley rats weighing from 220 to 250 g were used in the experiments. These animals were kept under laboratory standard conditions on a 12-h light/dark cycle, with light from 8:00 AM to 8:00 PM, in a temperature- (21–22°C) and humidity- (70%) controlled room. They were acclimatized for a minimum of 4 days before experiments were performed. Food (Standard Laboratory Rat, Mouse and Hamster diets; Panlab, Barcelona, Spain) and water were available ad libitum. The protocol of the study was approved by the Committee on Animal Experimentation of the University of Basque Country.

Surgical Procedure

The day before the experiment, the rats were lightly anesthetized with diethyl ether (Scharlau, Barcelona, Spain), and two polyethylene catheters (0.5 mm i.d., 11-cm-long; 0.3 mm i.d., 21-cm-long; Vygon, Ecouen, France) were implanted in the left jugular vein and right femoral artery for drug administration and blood sampling, respectively. The catheters were filled with physiological saline solution containing 1% heparin (50 I.U./ml; Roger Lab, Barcelona, Spain) to prevent clotting. These catheters were tunneled under the skin and exteriorized at the dorsal surface of the neck. Animals were housed individually in cages with free access to water.

Drug Analysis

The levels of (+)-M1 and (−)-M1 in plasma were determined by high-performance liquid chromatography with electrochemical detection (Valle et al., 1999). Briefly, plasma samples were spiked with 10 μl of internal standard followed by 200 μl of ammonium hydroxide. After the addition of 3 ml of ethyl acetate:*N*-hexane mixture (40:60, v/v), samples were shaken on a Vortex mixer for 2 min and centrifuged for 10 min at 3000 rpm. The organic phase was transferred to a 5-ml tube and evaporated down at vacuum in an Automatic Environmental Speed Vac evaporator (AES 100; Savant, Barcelona, Spain). The dried residues were reconstituted in 100 μl of deionized water, and an aliquot (50 μl) was injected into the chromatographic system.

The chromatographic system consisted of an HPLC 420 pump (Kontron Instruments, Barcelona, Spain) fitted with a manual sample injector (model 7125; Rheodyne, Barcelona, Spain) equipped with a 50-μl loop. Detection was performed with an ESA Coulochem model 5200 (ESA, Bedford, MA) electrochemical detector consisting of a model 5010 dual-electrode analytical cell (ESA) operating in the oxidation screening mode, with the potential of the first electrode set at +610 mV and the second electrode at +875 mV. Owing to the extreme flow sensitivity of the electrochemical detector, a pulse dampener was placed after the pump.

The analytical separation was performed by isocratic separation at room temperature, using an Asahipack ODP-50 column (5-μm particle size, 125- × 4.0-mm i.d.; Hewlett Packard, Palo Alto, CA). The mobile phase, consisting of 0.01 M borate buffer (pH = 9) and methanol (40:60, v/v), was filtered through a 0.22-μm membrane filter (Millipore Corp., Barcelona, Spain) and degassed by sonication. The flow rate was 0.7 ml/min; the mobile phase was recycled to conserve the solvents. The limit of quantification when 100 μl of plasma was used was 10 ng/ml; the signal showed linearity over the range 10 to 4000 ng/ml. The intra- and interday coefficients of variation of the assay were 5.5 and 8.5%, respectively.

(+)-M1 Experiments

Respiratory Depression Studies. Respiratory depression was studied in 20 rats randomly divided into five (n = 4) groups. The control group received a 10-min i.v. infusion of saline solution, and each of the other groups received 10-min i.v. infusions of (+)-M1 with 10, 5, 2.5, or 2 mg/kg, respectively. Arterial blood samples (100 μl) were collected in heparin-washed microtubes just before, during, and after the infusion was stopped at the following times: 0, 10, 15, 20, 25, 30, 40, 55, 70, 85, 100, 130, 160, and 250 min. The pH, pO_2, and pCO_2 levels were measured immediately by a blood gas analyzer (AVL 990; AVL Biomedical Instruments, Graz, Austria).

pk and Antinociceptive Studies. Animals (n = 33) were randomly divided into seven groups, each receiving a saline solution (three control groups) or a (+)-M1 infusion (groups I–IV) following the schedule represented in Table 1. The choice of the infusion rate

TABLE 1
Experimental protocol (doses and length of infusions) performed during the study describing the pharmacokinetic/pharmacodynamic relationships of (+)-M1

Group	n	Length of the Infusion	Dose
		min	*mg/kg*
I	6	10	2
II	6	10	0.7
III	6	60	2
IV	6	300	5.5
Control	3	10	0
Control	3	60	0
Control	3	300	0

for group I was based on the results obtained from the respiratory studies, and it included the highest dose avoiding changes in the respiratory parameters. The infusion rates given to groups II, III, and IV were calculated on the basis of the pk parameters obtained from group I.

Antinociception was determined, and arterial blood samples (50/100/200 μl) were withdrawn just before, during, and after the infusions were stopped as follows: group I, 0, 2.5, 5, 7.5, 10, 12.5, 15, 25, 40, 55, 70, 100, 130, 190, and 250 min; group II, 0, 1, 2.5, 5, 7.5, 10, 11, 12, 15, 20, 30, 40, 55, 70, 85, and 100 min; group III, 0, 5, 15, 30, 45, 60, 62.5, 65, 70, 90, 105, 120, 150, 180, and 240 min; group IV, 0, 5, 15, 30, 45, 60, 90, 120, 180, 240, 300, 305, 315, 330, 345, 360, 390, 420, 480, 540, 600, and 660 min.

The maximal total blood volume sampled was 1.9 ml. The same volume of extracted blood was reconstituted with heparinized physiological saline solution. Blood samples were transferred to heparinized tubes and were immediately centrifuged at 2500 rpm, 37°C, for 15 min to separate the plasma. Plasma was frozen and kept at −20°C until analysis was performed.

The effects of blood sampling (50–200 μl) and the duration of the infusion (10–300 min) on the antinociceptive effect were evaluated in the three control groups receiving saline solution. Antinociception was evaluated with the standard radiant heat tail-flick technique (D'Amour and Smith, 1941). Tail-flick latency was measured automatically with an Analgesic-Meter (Letica, Barcelona, Spain). The intensity of heat was adjusted so that basal latencies were 2 to 3 s; animals with higher baseline (>3–5 s) latencies were excluded from the study. A maximum cut-off time of 10 s was used to avoid tissue damage. Antinociception was expressed as a percentage of maximum possible effect (%MPE) and was calculated using the following expression:

$$\%\text{MPE} = \frac{\text{Test Latency} - \text{Baseline Latency}}{\text{Cut-off Time} - \text{Baseline Latency}} \cdot 100$$

β-FNA Studies. Male Sprague-Dawley rats ($n = 12$) were cannulated as described above. Two hours later, when the rats had recovered from the anesthesia, the antinociceptive baseline was measured, and a 10-mg/kg bolus dose of β-FNA was administered. Twenty-four hours after β-FNA administration, the rats were randomly divided into two groups receiving either 2 mg/kg (+)-M1 or saline solution in a 10-min i.v. infusion. Just before, during, and after the infusions were stopped, antinociception was determined, and arterial blood samples were withdrawn at the following times: 0, 2.5, 5, 7.5, 10, 12.5, 15, 25, 40, 55, 70, 100, and 130 min. The same volume of extracted blood was reconstituted with heparinized physiological saline solution. Blood samples were transferred to heparinized tubes and were immediately centrifuged at 2500 rpm, 37°C, for 15 min to separate the plasma. Plasma was frozen and kept at −20°C until analysis was performed.

(−)-M1 Experiments

pk and Antinociceptive Studies. Animals ($n = 12$) were randomly divided into two groups ($n = 6$). They received a 2- or 8-mg/kg dose of (−)-M1, respectively, in a 10-min i.v. infusion. Antinociception was determined as previously described for (+)-M1. Blood samples (50/100/200 μl) were collected at the start of the infusion and at 2.5, 5, 7.5, 10, 12.5, 15, 20, 30, 40, 55, 70, 90, 120, and 150 min thereafter. In the group receiving the higher dose, measurements were also performed at 180, 240, and 300 min. Blood samples were transferred to heparinized tubes and were immediately centrifuged at 2500 rpm, 37°C, for 15 min to separate the plasma. Plasma was frozen and kept at −20°C until analysis was performed.

Respiratory Depression Studies. Animals were randomly divided into two groups ($n = 4$) receiving 2 or 8 mg/kg of (−)-M1 in a 10-min i.v. infusion. Arterial blood samples (100 μl) were collected following the same scheme as described above for (+)-M1; pH, pO_2, and pCO_2 levels were determined.

Data Analysis

The time course of the plasma drug concentrations and antinociceptive effects was analyzed by population models using the first-order and first-order conditional estimation methods implemented in NONMEM (version V) software (Beal and Sheiner, 1992). This approach makes it possible to fit all data from all individuals simultaneously, describing both mean population tendencies and individual profiles, and providing estimates of the interindividual variability and residual (intraindividual) error. The residual error in the plasma drug concentrations and antinociceptive effects was characterized by proportional and additive error models, respectively:

$$C_{ij} = \text{Cpred}_{ij}(1 + \varepsilon\text{pk}_{ij})$$

$$E_{ij} = \text{Epred}_{ij} + \varepsilon\text{pd}_{ij}$$

where C_{ij} and E_{ij} are the jth observed plasma drug concentration and the antinociceptive response for the ith individual, respectively. Cpred_{ij} and Epred_{ij} are the jth model predicted plasma drug concentration and the antinociceptive response for the ith individual, respectively. ϵpk_{ij} and ϵpd_{ij}, the residual shift of the observations from the model predictions, are random variables assumed to be symmetrically distributed around 0 with variances σ^2_{pk} and σ^2_{pd}, respectively. Model predictions (Cpred_{ij} and Epred_{ij}) are based on the pk and pd models selected (see below) and on the estimates of individual parameters. For each parameter (P denotes an arbitrary pk or pd parameter), the expression for the ith individual is:

$$P_i = P_{\text{pop}} \cdot \exp(\eta_i)$$

where P_{pop}, the mean population estimate, and η_i, the shift of the parameter of the i^{th} individual from the population mean, are random variables assumed to be symmetrically distributed around 0 with diagonal variance-covariance matrix Ω with diagonal elements ($\omega_1^2, \ldots, \omega_m^2$). 1. . . m represent the pk or pd parameters to which interindividual variability has been assigned. During the analysis, P_{pop}, Ω, and σ^2 were estimated.

pk Analysis. Multicompartmental pk models were used to describe the kinetics of both (+)-M1 and (−)-M1 in plasma. Distribution processes were assumed to be linear. In the case of (+)-M1, a continuous increase in the plasma drug concentrations was seen during the infusion in group IV, apparently indicating nonlinearity in the elimination processes. This phenomenon was empirically modeled as a time-dependent decrease in total plasma clearance (Cl): $\text{Cl} = \text{Cl}_1 \cdot \exp(-\text{Cl}_2 \cdot \text{time})$, where Cl_1 and Cl_2 represent mean population parameters. Elimination of (−)-M1 was modeled as a linear process.

pd Analysis. To model the time course of the response and to overcome eventual model misspecifications occurring during the pk analysis, the plasma drug concentration versus time profiles for each animal were modeled nonparametrically with linear interpolation. When the antinociceptive effect was plotted against the plasma concentration in a time-ordered manner, counterclockwise hysteresis was seen for all animals. This phenomenon suggests (among other possible explanations) a time delay for (+)-M1 in plasma to equilibrate with the biophase. Such a delay has been modeled by linking plasma drug concentrations with effect site concentrations (C_e) by means of a first-order rate constant (k_{e0}; Sheiner et al., 1979). Linear, $E_{\max}$, and sigmoidal $E_{\max}$ models were explored to describe the pd (effect versus C_e) relationship. This analysis shows that the pd parameters of (+)-M1 depended on the length of the infusion, which could be interpreted as a development of tolerance. Therefore, models accounting for tolerance development (Porchet et al., 1988; Ekblom et al., 1993; Mandema and Wada, 1995) were also fitted to the data.

Model selection was based on the exploratory analysis of goodness-of-fit plots performed with the Xpose package (Jonsson and Karlsson, 1999), the estimates of the parameters, and their confidence intervals. The minimum value of the objective function provided by

NONMEM was also used as a criterion for model selection. The difference in the objective function between two hierarchical models is approximately χ^2 distributed; $P < .05$ was used as the level of significance. Results from the data analysis are presented as estimated values and their coefficients of variation [c.v. (%)]. Estimates of the interindividual and residual variability are expressed as c.v. (%).

Statistical Analysis

Results from the respiratory effects and antinociception for the β-FNA experiments were represented as mean data with their corresponding standard deviations. Comparisons among groups were made by one-way ANOVA followed by the Scheffe's *F* test. Statistical significance was set at $P < .05$.

Results

(+)-M1 Experiments

Respiratory Depression. (+)-M1, administered as an i.v. infusion for 10 min, elicited a dose-dependent respiratory depression characterized by a decrease in the arterial pH and pO_2 and an increase in arterial pCO_2 levels (Fig. 1). Although the pH levels decreased from a mean baseline value of 7.5 to minimum values of 7.43, 7.39, 7.37, and 7.22 after the administration of the 2-, 2.5-, 5-, and 10-mg/kg dose, respectively, only the decrease observed after the highest dose was found to be statistically significant ($P < .05$).

Time to maximum pH response depends also on the administered dose. It ranged from 25 min in the 2.5-mg/kg dose group to 40 to 55 min in the 10-mg/kg dose group. The time for returning to baseline was approximately 100 min for the 2.5- and 5-mg/kg dose groups and 200 min for the highest studied dose.

Similar patterns were seen for pO_2 and pCO_2 measures. After the administration of the higher dose, pO_2 levels showed a statistically significant ($P < .05$) decrease of 32 mm Hg with respect to baseline, and pCO_2 levels showed a statistically significant increase ($P < .05$) of 32 mm Hg with respect to baseline. Time to peak response increased again with the administered dose, and no rebound effects were found. pCO_2 returned to baseline 120 min after the administration of the highest dose, whereas for pO_2, the time to baseline was ~250 min (see Fig. 1).

pk. The mean observed plasma concentrations of (+)-M1 versus time profiles for groups I to IV are represented in Fig. 2. Maximum mean observed plasma drug concentrations were 639.2 ± 299.6, 187.54 ± 79.5, 208.62 ± 36.7, and 261.4 ± 37.2 ng/ml for groups I to IV, respectively.

Figure 2 also shows the time course of the mean population predictions. Drug disposition was best described by a two-compartmental model. Describing the elimination of (+)-M1 as a function dependent on the time after the start of the infusion significantly improved the fit ($P < .01$). Estimates of fixed and random parameters are listed in Table 2. No covariate effects of the total administered dose or the length of infusion were found. Interindividual variability could only be estimated in total clearance and initial volume of distribution, resulting in 23 and 55%, respectively.

pk/pd Analysis of the Antinociceptive Effect. When saline was administered in infusions of 10, 60, or 300 min, no antinociception was observed. The %MPE ranged between 0 and 29%. Baseline antinociceptive measurements did not differ statistically ($P > .05$) between control and drug-treated groups.

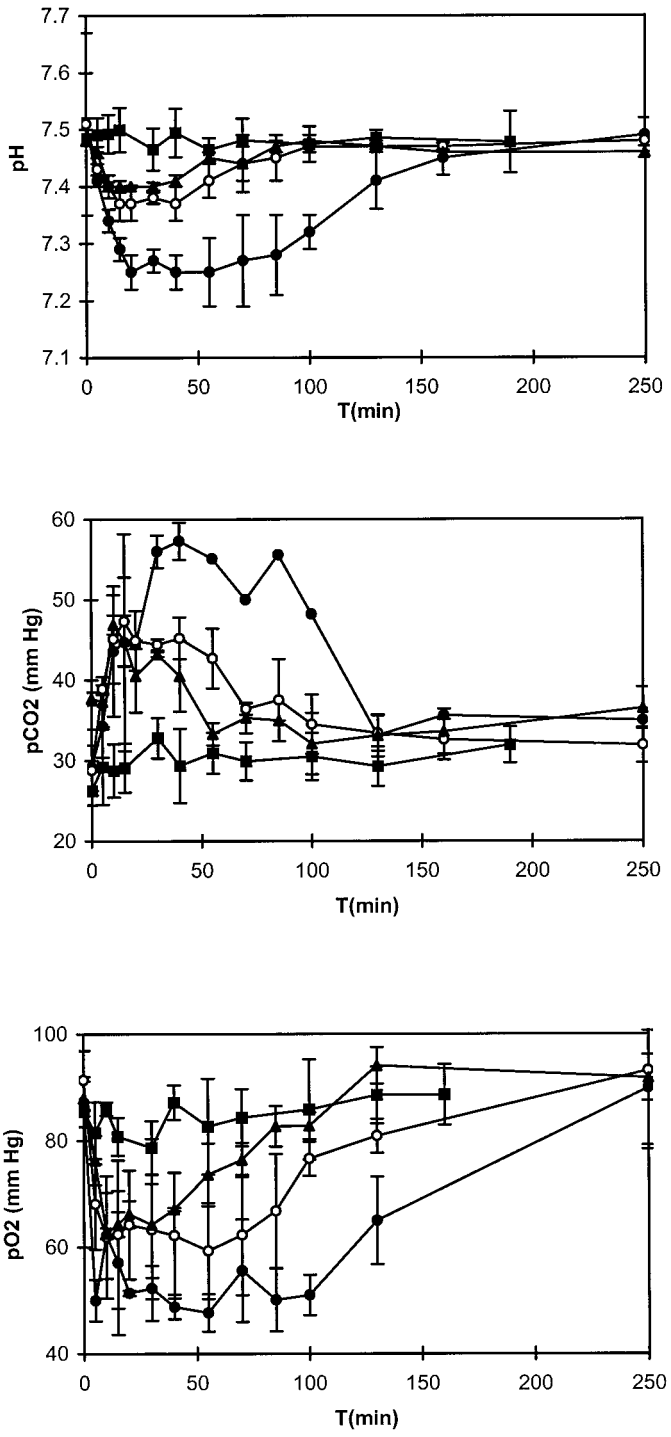

Fig. 1. Time course of arterial pH (upper panel), pCO_2 (middle panel), and pO_2 (lower panel) after the administration of saline (■), 10 (●), 5 (○), or 2.5 (▲) mg/kg (+)-M1 in 10-min i.v. infusions. Points represent the mean data and vertical lines represent the standard deviations.

The time course of the antinociception in groups I to IV is shown in Fig. 3. The mean peak observed effect in groups I and III was 100%. For groups II and IV, the maximum observed effect was 42.9 and 90.5%, respectively. Time to peak was 15 min for groups I and II. Time to peak for groups III and IV occurred at the end of the infusion (60 and 300 min, respectively).

Antinociception versus effect site concentrations was best

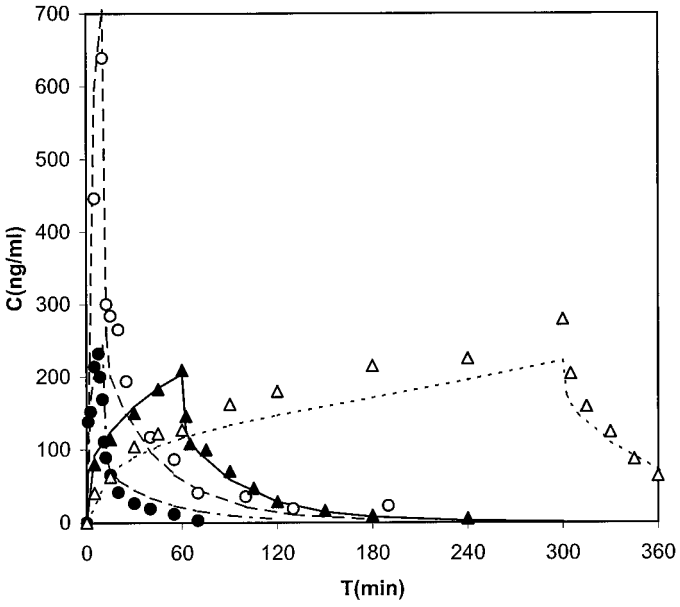

Fig. 2. Time course of the plasma concentrations of (+)-M1. Points represent mean observed data for groups I (○), II (●), III (▲), and IV (△). Lines represent mean population model predictions for groups I (— —), II (--), III (- - -), and IV (- -). Standard deviations have been omitted for clarity.

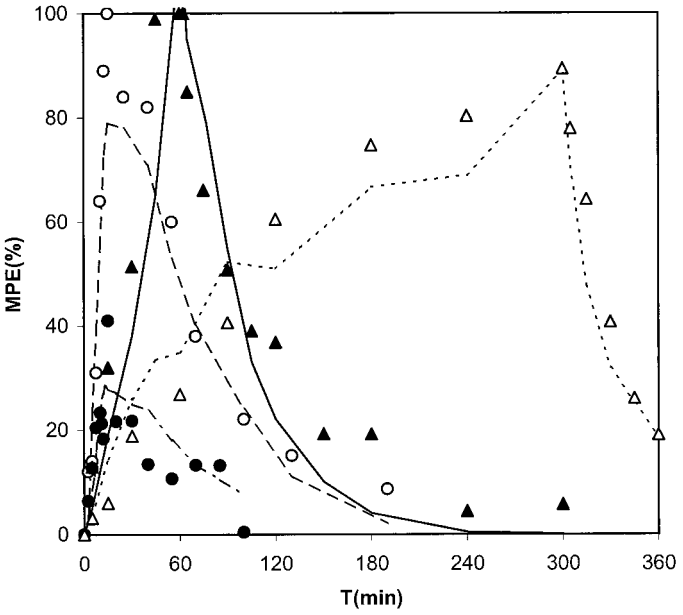

Fig. 3. Time course of %MPE after (+)-M1 administration. Points represent mean observed data for groups I (○), II (●), III (▲), and IV (△). Lines represent mean population model predictions for groups I (— —), II (--), III (- - -), and IV (- -). Standard deviations have been omitted for clarity.

TABLE 2

Pharmacokinetic parameter estimates of (+)-M1

Estimates of interindividual variability are expressed as c.v. (%). Precision of the estimates is expressed as relative standard error in parentheses. Relative standard error is standard error divided by the parameter estimate.

Parameter	Estimate	IIV
V_c (l)	0.100 (0.33)	55 (0.65)
V_{SS} (l)	0.781 (0.08)	NE
Cl_d (l/min)	0.0563 (0.12)	NE
$Cl = Cl_1 \cdot \exp(-Cl_2 \cdot time)$ (l/min)	Cl_1 = 0.035 (0.07)	23 (0.42)
	Cl_2 = 0.0023 (0.17)	

V_c, initial volume of distribution; V_{SS}, apparent volume of distribution at steady state; Cl_d, intercompartmental clearance; IIV, interindividual variability; NE, not estimated in the model.

modeled by a linear pharmacodynamic model. A significantly ($P < .001$) better fit was obtained when different typical values for k_{e0} and slope were estimated for each group, compared with the model using the same typical value for k_{e0} and slope in all groups. Table 3 lists the estimates of k_{e0} and slope for each of the groups. There is a clear tendency for k_{e0} to increase and for slope to decrease with the length of the infusions. Although different models allowing for tolerance development were fitted to the data (see *Materials and Methods*), none of them gave adequate predictions or reasonable parameter estimates.

β-FNA Experiments. The pretreatment with 10 mg/kg β-FNA did not alter the baseline antinociception; however, as is represented in Fig. 4, β-FNA pretreatment antagonized completely the antinociceptive effect of the 2-mg/kg dose of (+)-M1 administered in a 10-min i.v. infusion, the maximum mean observed effect being 11.7%. pk parameters of (+)-M1 in rats pretreated with β-FNA did not differ ($P > .05$) from those obtained for groups I to IV (data not shown).

(−)-M1 Experiments

Figure 5 shows the pk profiles of (−)-M1 after the administration of a 2- or 8-mg/kg dose in 10-min i.v. infusions. The disposition of (−)-M1 in plasma was best described by a two-compartmental model. pk behavior was different between the two administered dose groups. Differences affected initial volume of distribution and total plasma clearance. Table 4 lists the estimates of the pk parameters.

Antinociceptive and respiratory measurements were recorded during and after the infusion of (−)-M1. However, no significant changes ($P > .05$) from baseline were detected in either effect (data not shown).

Discussion

Tramadol is a centrally acting analgesic drug with several potentially complicating pk/pd factors that could make the interpretation of the time course of antinociception difficult. In fact, to our knowledge nothing describing its pk/pd relationships has been published. These factors include: 1) Kinetic disequilibrium between plasma and biophase (central nervous system). Several authors have reported delays between plasma and the effect compartment for several opioid drugs, such as morphine (Ekblom et al., 1993), methadone (Garrido et al., 1999), and alfentanyl (Mandema and Wada, 1995). 2) Tolerance development. This phenomenon has also been observed and quantified for opioid drugs such as morphine (Ouellet and Pollack, 1995, Gårdmark et al., 1993) and alfentanyl (Mandema and Wada, 1995). 3) Pharmacodynamic interactions. Tramadol is administered as a racemic mixture of two active enantiomers (Raffa et al., 1993), and, consequently, interactions are expected to be present. In addition, each of the enantiomers forms active metabolites (Paar et al., 1992) that could modify these interactions or make them more complex.

The aim of this work is the analysis of the pk/pd relationships of the two main active metabolites, (+)-M1 and (−)-M1, because there are some indications that suggest they might play a significant role in the analgesic effect of tramadol (Raffa and Friderichs, 1996). Both metabolites were admin-

TABLE 3
Pharmacodynamic parameter estimates of (+)-M1
Estimates of interindividual variability are expressed as c.v. (%). Precision of the estimates is expressed as relative standard error in parenthesis. Relative standard error is standard error divided by the parameter estimate.

	Group I	Group II	Group III	Group IV	IIV
k_{e0} (1/min)	0.03 (0.10)	0.02 (0.50)	0.05 (0.56)	0.28 (1.40)	0.13 (0.69)
Slope (% ml/ng)	0.53 (0.075)	0.58 (0.41)	0.41 (0.12)	0.33 (0.18)	0.68 (0.05)

k_{e0}, first-order rate constant of equilibrium between plasma and effect compartment; IIV, interindividual variability.

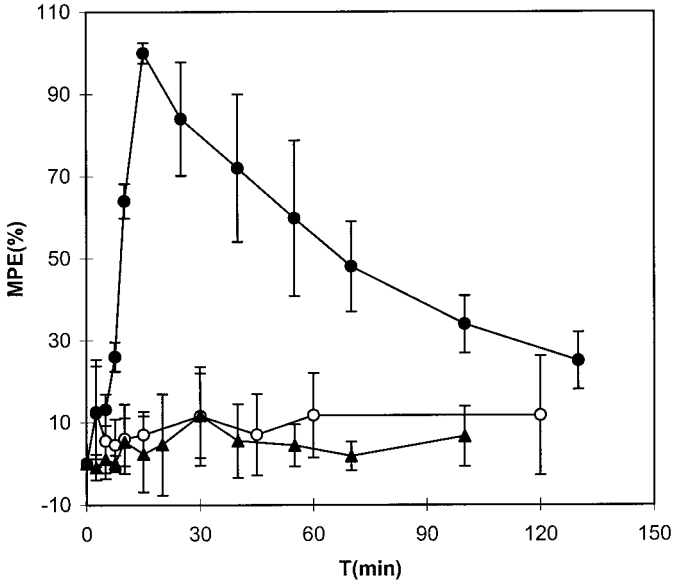

Fig. 4. Time course of the antinociceptive effect after saline administration (○), 2 mg/kg (+)-M1 in 10-min i.v. infusion (●), and 2 mg/kg (+)-M1 in 10-min i.v. infusion in the β-FNA pretreated group (▲). Points represent mean observed data and vertical lines represent standard deviations.

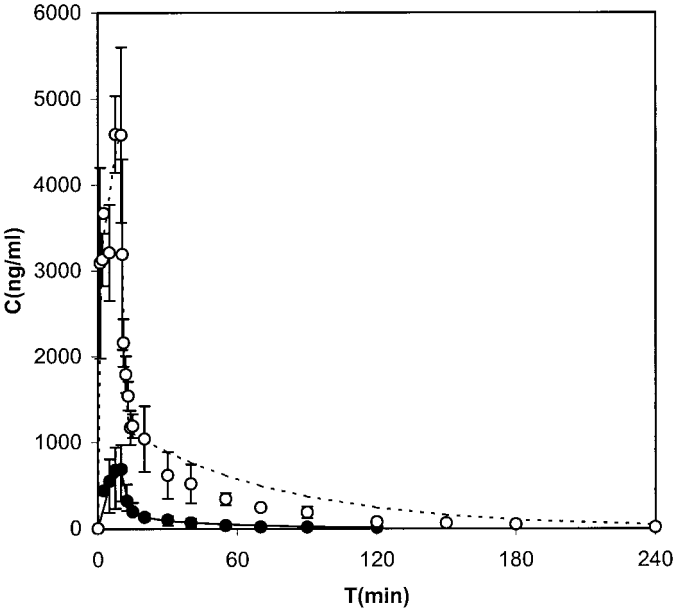

Fig. 5. Time course of the plasma concentrations of (−)-M1. Points represent mean observed data with standard deviations for the 2- (●) and 8-mg/kg (○) dose groups. Lines represent mean population model predictions: solid (2 mg/kg) and dashed (8 mg/kg).

istered separately because this type of design offers the advantage of obtaining direct information about the pk and pd properties of the metabolites, and this design has been previously used for other drugs with active metabolites like midazolam (Mandema et al., 1992).

TABLE 4
Pharmacokinetic parameter estimates of (−)-M1
Estimates of interindividual variability are expressed as c.v. (%). Precision of the estimates is expressed as relative standard error in parentheses. Relative standard error is standard error divided by the parameter estimate.

Parameter	Estimate	IIV
$V_{c(1)}$ (l)	0.255 (0.23)	0.58 (0.67)
$V_{c(2)}$ (l)	0.05 (0.18)	
V_{SS} (l)	0.72 (0.07)	NE
Cl_d (l/min)	0.036 (0.14)	NE
$Cl_{(1)}$ (l/min)	0.0395 (0.07)	0.84 (0.47)
$Cl_{(2)}$ (l/min)	0.0156 (0.05)	

(1) and (2) refer to 2- and 8-mg/kg doses, respectively. V_c, initial volume of distribution; V_{SS}, apparent volume of distribution at steady state; Cl_d, intercompartmental clearance; IIV, interindividual variability; NE, not estimated in the model.

(+)-M1 Experiments. (+)-M1 was administered at different rates in i.v. infusions of different lengths. This procedure is similar to that used by Gårdmark et al. (1993) to evaluate the pk/pd properties of morphine. The tail-flick test has been shown to be appropriate for characterizing in vivo responses associated with the interaction of agonists with the μ-receptor, as has been reported for buprenorphine (Ohtani et al., 1995), methadone (Garrido et al., 1999), and morphine (Ouellet and Pollack, 1997).

The doses given during the pk/pd analysis of the antinociceptive response were chosen on the basis of the results of the respiratory depression experiments and were those with no associated respiratory effects. It was found that doses lower than 2 mg/kg given in a 10-min i.v. infusion were unlikely to have respiratory effects. Doses higher than 2.5 mg/kg, administered by short i.v. infusion (10 min), produced dose-dependent respiratory depression characterized by a decrease in pH and pO_2 levels and an increase in pCO_2 levels. Comparison of the results of this study with data from other opioids showed that 10 mg/kg (+)-M1 administered in 10-min i.v. infusion elicits an alteration in the respiratory parameters similar to 7.5 mg/kg methadone administered as an i.p. injection (White and Zagon, 1979) or to 3 mg/kg norbuprenorphine (active metabolite of buprenorhine) administered as an i.v. bolus (Ohtani et al., 1997).

(+)-M1 kinetics in plasma was best described with a two-compartmental model. The distribution phase was fast (distribution half-life = 1.2 min) and linear over the dose range studied. However, clearance showed a slight decrease in time after the start of the infusion. A similar pattern has been described previously for other opioids administered in long infusions. Ekblom et al. (1993) and Gårdmark et al. (1993) observed that total plasma clearance of morphine decreased after long infusions when compared with those estimated from short infusions or bolus data. In our study, because maximum plasma drug concentrations were similar for groups II, III, and IV, the decrease in clearance could not be

explained by a concentration-dependent process. This finding could be related to the fact that there is a possibility for higher respiratory effects during the 300-min infusion than during the 10- or 60-min infusions; however, the effect of respiratory depression on the elimination of (+)-M1 has not been established yet.

The 20-min estimate of the mean population terminal half-life obtained in this study differs from the 4.23-h estimate reported previously by Takacs (1995). Because the administered drug was tramadol in that study, those differences suggest that the rate of elimination of (+)-M1 is limited by its rate of formation from the parent compound.

The pk/pd analysis of the antinociceptive effect suggests tolerance development because the estimates of k_{e0} and slope increase and decrease, respectively, with the length of the infusion (Table 3). In addition, for the two 10-min infusions, the one associated with higher plasma drug concentrations (group I) corresponds to a higher k_{e0} and lower slope values. These results indicate that development of tolerance depends on total drug exposure. Although a priori, our experimental design was appropriate to account for development of tolerance, owing to the fact that during the longer infusion plasma drug concentrations were continuously increasing, such a phenomenon could not be adequately quantified.

The value of mean population estimates of k_{e0} (0.03/min) for the 10-min lowest dose infusion group (no, or minor tolerance development) was lower than the value estimated for methadone (1.44/min; Garrido et al., 1999), similar to that estimated for morphine (0.073/min; Ouellet and Pollack, 1995), and higher than those described for morphine-6-glucuronide (0.005/min; Gårdmark and Hammarlund-Udenaes, 1998) and morphine (0.02/min; Gårdmark et al., 1993). These differences could be explained by differences in liposolubility between the drugs (Dutta et al., 1998).

Recently, Grond et al. (1999) determined the plasma concentrations of the enantiomers of tramadol and M1 metabolite following an i.v. bolus dose of 200 mg and demand doses of 20 mg. It was found that the mean (+)-M1 plasma drug concentration before demand was 57 ng/ml, so (+)-M1 plasma concentrations were probably well above 57 ng/ml at times near drug administration. Taking into account that our experiments showed that (+)-M1 steady-state plasma drug concentrations of 200 ng/ml elicit near maximal antinociception, (+)-M1 could be expected to have a role in the analgesic effect of tramadol. However, additional studies are required to characterize the nature of the tramadol/(+)-M1 interaction in humans.

β-FNA is a μ-selective irreversible antagonist that produces a long-lasting antagonism of several behavioral effects of μ-agonist. However, it does not antagonize the effects of drugs acting at κ- or δ-opioid receptors (Pitts et al., 1998). Generally, the antagonism of β-FNA evidences the fact that a given behavioral effect of a drug involves actions on μ-opioid receptors. The insurmountable antagonism of β-FNA on the antinociceptive effect elicited by (+)-M1 supports the results from in vitro studies where (+)-M1 showed a moderate affinity for μ-opioid receptors: K_i = 153 nM (Lai et al., 1996), and shows that the behavior of (+)-M1 in the antinociceptive test is mediated by μ-opioid receptors. Similar results were reported by Randich et al. (1993) for a 1-mg/kg i.v. dose of morphine given 24 h after pretreatment with a 10-mg/kg i.v. bolus of β-FNA in rats, using the tail-flick reflex test.

(−)-M1 Experiments. The kinetics of (−)-M1 was best described using a two-compartmental model. The 4-fold differences found in total clearance and initial volume of distribution between the two doses used in the current study could explain dose-dependent distribution and elimination kinetics. The pk estimates obtained from the analysis of the lower-dose group were similar to those obtained during the pk analysis of the (+)-M1 data, suggesting that, after administration of low doses, both enantiomers have similar kinetics.

(−)-M1 presents a very low affinity for opioid receptors (Lai et al., 1996), its main action being due to the inhibition of the NA uptake (Driessen et al., 1993). As was expected on the basis of the in vitro properties of (−)-M1, no antinociceptive effect in the tail-flick test or respiratory depression was observed after the administration of this compound in this study, despite the high administered doses. Several in vivo studies have reported an important contribution by the non-opiate component of tramadol in its antinociception because a peripheral administration of the alpha$_2$-adrenergic antagonists, such as yohimbine, blocked partially its antinociceptive effect (Raffa et al., 1995). In addition, the potentiation of opioid analgesia by NA uptake blockers and α_2-agonists is documented in clinical and preclinical findings, although there is no consensus about the intrinsic antinociceptive effect of these compounds on their own (Sevcik et al., 1993; Codd et al., 1995). In this case, the (−)-M1, a compound with the property to inhibit NA uptake, did not induce either antinociceptive effect in the tail-flick test or adverse effects such as respiratory depression.

In conclusion, this study represents the first pk/pd analysis of the two main active metabolites of tramadol. The pharmacokinetics of both compounds can be considered similar and is well described with multicompartmental models. Antinociceptive response elicited by (+)-M1 could be described by standard pk/pd models and was mediated by μ-opioid receptor activation. In our results we found evidence for the development of tolerance. Respiratory effects were observed at higher doses than the ones given the maximum antinociception. (−)-M1 showed neither antinociception in the tail-flick test nor respiratory effects. Further studies are required to account for the interaction of both compounds given simultaneously.

Acknowledgments

We thank Professor José M. Baeyens for critical review of the pharmacodynamic concepts and Professors Mats O. Karlsson and Margareta Hammarlund-Udenaes for suggestions regarding the pharmacokinetic/pharmacodynamic data analysis. The generous gift of (+)-*O*-desmethyltramadol, (−)-*O*-desmethyltramadol, and ethoxy analog of tramadol by Grünenthal GmbH is greatly appreciated.

References

Adams JU, Paronis CA and Holtzman SG (1990) Assessment of relative intrinsic activity of m-opioid analgesics in vivo by using β-funaltrexamine. *J Pharmacol Exp Ther* **255:**1027–1032.

Bamigbade TA, Davidson C, Langford RM and Stamford JA (1997) Actions of tramadol, its enantiomers and principal metabolite, *O*-desmethyltramadol, on serotonin (5-HT) efflux and uptake in the rat dorsal raphe nucleus. *Br J Anaesth* **79:**352–356.

Beal SL and Sheiner LB eds (1992) *NONMEM Users Guides*. NONMEM Project Group, University of California at San Francisco, San Francisco, CA.

Codd EE, Shank RP, Schupsky JJ and Raffa RB (1995) Serotonin and norepinephrine uptake inhibiting activity of centrally acting analgesics: Structural determinants and role in antinociception. *J Pharmacol Exp Ther* **274:**1263–1270.

Derendorf H and Hochhaus G (1995) *Handbook of Pharmacokinetic/Pharmacodynamic Correlation*. CRC Press, Boca Raton, FL.
D'Amour FE and Smith DL (1941) A method for determining loss of pain sensation. *J Pharmacol Exp Ther* **72:**74–79.
Driessen B, Reimanan W and Giertz H (1993) Effects of the central analgesic tramadol on the uptake and release of noradrenaline and dopamine in vitro. *Br J Pharmacol* **108:**806–811.
Dutta S, Matsumoto Y, Muramatsu A, Matsumoto M, Fukuoka M and Ebling WF (1998) Steady-state propofol brain:plasma and brain:blood partition coefficients and the effect-site equilibration paradox. *Br J Anaesth* **81:**422–424.
Ekblom M, Hammarlund-Udenaes M and Paalzow L (1993) Modeling of tolerance development and rebound effect during different intravenous administrations of morphine to rats. *J Pharmacol Exp Ther* **266:**244–252.
Frink MC, Hennies HH, Englberger W, Haurand M and Wilffert B (1996) Influence of tramadol on neurotransmitter systems of the rat brain. *Arzneim-Forsch* **46:** 1029–1036.
Gårdmark M, Ekblom M, Bouw R and Hammarlund-Udenaes M (1993) Quantification of effect delay and acute tolerance development to morphine in the rats. *J Pharmacol Exp Ther* **267:**1061–1067.
Gårdmark M and Hammarlund-Udenaes M (1998) Delayed antinociceptive effect following morphine-6-glucuronide administration in the rat-pharmacokinetic/pharmacodynamic modelling. *Pain* **74:**287–296.
Garrido MJ, Valle M, Calvo R and Trocóniz IF (1999) Altered plasma and brain disposition and pharmacodynamics of methadone in abstinent rats. *J Pharmacol Exp Ther* **288:**179–187.
Grond S, Meuser T, Uragg H, Stahlberg HJ and Lehmann KA (1999) Serum concentrations of tramadol enantiomers during patient-controlled analgesia. *Br J Clin Pharmacol* **48:**254–257.
Hennies HH, Friderichs E and Schneider J (1988) Receptor binding, analgesic and antitussive potency of tramadol and other selected opioids. *Arzneim-Forsch* **38:** 877–880.
Houmes RJM, Voets MA, Verkaaik A, Erdmann W and Lachmann B (1992) Efficacy and safety of tramadol versus morphine for moderate and severe postoperative pain with special regard to respiratory depression. *Anesth Analg* **74:**510–514.
Hummel T, Roscher S, Pauli E, Frank M, Liefhold J, Fleischer W and Kobal G (1996) Assessment of analgesia in man: Tramadol controlled release formula vs tramadol standard formulation. *Eur J Clin Pharmacol* **51:**31–38.
Jonsson EN and Karlsson MO (1999) Xpose: An S-PLUS based population pharmacokinetic/pharmacodynamic model building aid for NONMEM. *Comput Methods Programs Biomed* **58:**51–64.
Lai J, Ma S, Porreca F and Raffa RB (1996) Tramadol, M1 metabolite and enantiomer affinities for cloned human opioid receptors expressed in transfected HN9.10 neuroblastoma cells. *Eur J Pharmacol* **316:**369–372.
Lee CR, McTavish D and Sorkin EM (1993) Tramadol: A preliminary review of its pharmacodynamic and pharmacokinetic properties, and therapeutic potential in acute and chronic pain states. *Drugs* **46:**313–340.
Mandema JW, Tuk B, Van Steveninck AL, Breimer DD, Cohen A and Danhof M (1992) Pharmacokinetic-pharmacodynamic modelling of the central nervous system effects of midazolam and its main metabolite α-hydroxymidazolam in healthy volunteers. *Clin Pharmacol Ther* **51:**715–728.
Mandema JW and Wada DR (1995) Pharmacodynamic model for acute tolerance development to the electroencephalographic effects of alfentanil in the rat. *J Pharmacol Exp Ther* **275:**1185–1194.
Miranda HF and Pinardi G (1998) Antinociception, tolerance and physical dependence comparison between morphine and tramadol. *Pharmacol Biochem Behav* **61:**357–360.
Ohtani M, Kotaki H, Sawada Y and Iga T (1995) Comparative analysis of buprenorphine- and norbuprenorphine-induced analgesic effects based on pharmacokinetic-pharmacodynamic modelling. *J Pharmacol Exp Ther* **272:**505–510.
Ohtani M, Kotaki H, Nishitateno K, Sawada Y and Iga T (1997) Kinetics of respiratory depression in rats induced by buprenorphine and its metabolite, norbuprenorphine. *J Pharmacol Exp Ther* **281:**428–433.
Ouellet DMC and Pollack GM (1995) A pharmacokinetic-pharmacodynamic model of tolerance to morphine analgesia during infusion in rats. *J Pharmacokinet Biopharm* **23:**531–549.
Ouellet DMC and Pollack GM (1997) Pharmacodynamics and tolerance development during multiple intravenous bolus morphine administration in rats. *J Pharmacol Exp Ther* **281:**713–720.
Paar WD, Frankus P and Dengler HJ (1992) The metabolism of tramadol by human liver microsomes. *Clin Investig* **70:**708–710.
Pitts RC, Allen RM, Walker EA and Dykstra LA (1998) Clocinnamox antagonism of antinociceptive effects of mu opioids in Squirrel monkeys. *J Pharmacol Exp Ther* **285:**1197–1206.
Porchet HC, Benowitz NL and Sheiner LB (1988) Pharmacodynamic model of tolerance: Application to nicotine. *J Pharmacol Exp Ther* **244:**231–236.
Raffa RB and Friderichs E (1996) The basic science aspect of tramadol hydrochloride. *Pain Rev* **3:**249–271.
Raffa RB, Friderichs E, Reimann W, Shank RP, Codd EE and Vaught JL (1992) Opioid and nonopioid components independently contribute to the mechanism of action of tramadol, an "atypical" opioid analgesic. *J Pharmacol Exp Ther* **260:**275–285.
Raffa RB, Friderichs E, Reimann W, Shank RP, Codd EE, Vaught JL, Jacoby HI and Selve N (1993) Complementary and synergistic antinociceptive interaction between the enantiomers of tramadol. *J Pharmacol Exp Ther* **267:**331–340.
Raffa RB, Nayak RK, Liao S and Minn FL (1995) The mechanism(s) of action and pharmacokinetics of tramadol hydrochloride. *Rev Contemp Pharmacother* **6:**485–497.
Randich A, Robertson JD and Willingham T (1993) The use of specific opioid agonists and antagonists to delineate the vagally mediated antinociceptive and cardiovascular effects of intravenous morphine. *Brain Res* **603:**186–200.
Sheiner LB, Stanski DR, Vozeh S, Miller RD and Ham J (1979) Simultaneous modelling of pharmacokinetics and pharmacodynamics: Application to d-tubocuranine. *Clin Pharmacol Ther* **25:**358–371.
Sevcik J, Nieber K, Driessen B and Illes P (1993) Effects of the central analgesic tramadol and its main metabolite, O-desmethyltramadol, on rat locus coeruleus neurones. *Br J Pharmacol* **110:**169–176.
Takacs AR (1995) Ancillary approaches to toxicokinetic evaluations. *Toxicol Pathol* **23:**179–186.
Valle M, Pavón JM, Calvo R, Campanero MA and Trocóniz IF (1999) Simultaneous determination of tramadol and its major active metabolite O-demethyltramadol by High-Performance Liquid Chromatography with electrochemical detection. *J Chromatogr B Biomed Sci Appl* **724:**83–89.
White WJ and Zagon IS (1979) Acute and chronic methadone exposure in adult rats: Studies on arterial blood gas concentrations and pH. *J Pharmacol Exp Ther* **188:**451–455.

Send reprint requests to:Iñaki F. Trocóniz PhD, Department of Pharmacy and Pharmaceutical Technology, Faculty of Pharmacy, University of Navarra, Pamplona 31080, Spain. E-mail: itroconiz@unav.es.